NJC

Accepted Manuscript

This is an *Accepted Manuscript*, which has been through the Royal Society of Chemistry peer review process and has been accepted for publication.

Accepted Manuscripts are published online shortly after acceptance, before technical editing, formatting and proof reading. Using this free service, authors can make their results available to the community, in citable form, before we publish the edited article. We will replace this *Accepted Manuscript* with the edited and formatted *Advance Article* as soon as it is available.

You can find more information about *Accepted Manuscripts* in the Information for Authors.

Please note that technical editing may introduce minor changes to the text and/or graphics, which may alter content. The journal's standard Terms & Conditions and the Ethical guidelines still apply. In no event shall the Royal Society of Chemistry be held responsible for any errors or omissions in this *Accepted Manuscript* or any consequences arising from the use of any information it contains.

ROYAL SOCIETY OF CHEMISTRY

www.rsc.org/njc

NJC

RSCPublishing

PAPER (or FOCUS or PERSPECTIVE)

Preparation of *n*-Type Semiconducting Polymer Nanoarrays by Covalent Synthesis Followed by Crystallization

Cite this: DOI: 10.1039/c3nj00000x

Received 00th XXXXX 2013,
Accepted 00th XXXXX 2013

DOI: 10.1039/c3nj00000x

www.rsc.org/njc

Begum, Fouzia[a], John Ferguson[a], Kelly McKenna[a], Louis E. McNamara[b], Nathan I. Hammer[b*], and Hemali Rathnayake[a*]

In-situ covalent synthesis followed by solution crystallization of the n-type semiconducting polymer derived from pereylenediimide-bridged silsesquioxanes (PDIB-SSQ) yielded 1D-nanoarrays of 40-100 nm widths and up to 80 μm lengths. Morphologies and dimensions of nanostructures resulting from different base concentrations were characterized by SEM, fluorescence optical microscopy, SAXS, elemental analysis, MALDI-TOF-MS, and absorption and fluorescence spectroscopies. As revealed by SAXS, the nanostructures are composed of crystalline unit cells with cell parameters of $d_{[001]}$ = 24.8 Å and $d_{[100]}$ = 10.3 with multiple π-π stacking distances ranging from 4.71 to 2.57 Å. The ordering in polymer nanoarrays is favoured by the π-π interactions between the cofacially arranged PDI cores, resulting closely packed polymer arrays with the d-spacing ranging from 3.67 Å to 3.24 Å. The spectroscopic traces of nanoarrays in solution resembled that of the monomer except the slightly red shifted features of the emission spectrum associated with π-π stacking of polymer chains in aggregated form. Thin film emission spectra followed the similar spectral pattern with a noticeable shoulder corresponds to cofacial π-π interactions. The excited state lifetimes of aggregated polymer nanoarrays in both solution and solid phase were nearly identical. The electrical characterization of thin films made from polymer nanoarrays shows typical semiconducting behaviour with the electrical conductivity of 0.48 x 10^{-3} S/cm. The covalent synthesis followed by solution-based crystallization of PDIB-SSQ reported herein provides a new synthesis path to make ordered-crystalline semiconducting polymer nanoarrays and ultimately benefits for better understanding of their role in organic electronics.

Introduction

Aromatic molecules derived from fused-arenes are a common class of organic semiconductors known to form one-dimensional (1D) nanostructures through strong π-π interactions.[2-13] The concept of self-assembly is the most widely used method to make such nanostructures for designing electronic and optoelectronic devices. A variety of self-assembled nanostructures derived from aromatic molecules including porphyrines,[2] hexathiapentacenes,[4] triphenylenes,[5] phthalocynanines,[6] oligoacenes,[7] and perylenetetracarboxylic diimide derivatives[8-12] has been prepared by molecular self-assembly processes using non-covalent interactions.

P-type and n-type organic semiconducting materials have gained tremendous scientific interest due to their unique electronic properties and have been widely applied in organic field effect transistors (OFETs), organic light emitting diodes (OLEDs), and organic-based photovoltaics (OPVs).[14-18] However, organic based thin-film devices such as bulk heterojunction solar cells are strongly dependent on the organization of the n- and p- type materials and their molecular interactions with the substrates.[15-18] To improve the efficiency of these optoelectronic devices, it is essential to have well-defined nanoarrays with guidable self-assembly properties.

Significant research efforts have been contributed to self-assembling p-type semiconductors when compared to n-type semiconductors.[13] N-type materials are more demanding in creating ordered networks with p-type semiconductors for electronic device applications especially for OPVs. Among n-type semiconductors, self-organized perylenediimides (PDIs) are widely studied because of their promising optoelectronic properties as well as their propensity to form 1D nanostructures through strong π-π interactions.[19-22] The self-assembled 1D-structures of PDIs such as nanowires,[5,22,23] nanobelts,[8,9] nanotubes,[10,11] and nanofibres[12] were introduced through a variety of techniques such as phase transfer, solvent annealing, vapour diffusion, and seeded growth. However, these self-organization processes have limited control on achieving

nanosized structures with distinct geometries. It has been shown that covalent synthesis is an alternative path to make organized nanostructures with controlled morphologies.[24,25] Nonetheless, reports to date on preparing ordered nanostructures from semiconducting polymers are very limited.[26-28] Here, we report an in-situ base-catalyzed hydrolysis and condensation method to prepare crystalline nanoarrays of polymeric perylenediimide-bridged silsesquioxanes (Poly-PDIB-SSQ). These nanoarrays of poly-PDIB-SSQ were characterized by elemental analysis, MALDI-TOF-MS, FT-IR, scanning electron microscopy (SEM), fluorescence optical microscopy, small angle X-ray powder scattering (SAXS), and solution and thin film absorption and fluorescence spectroscopies.

Results and Discussion

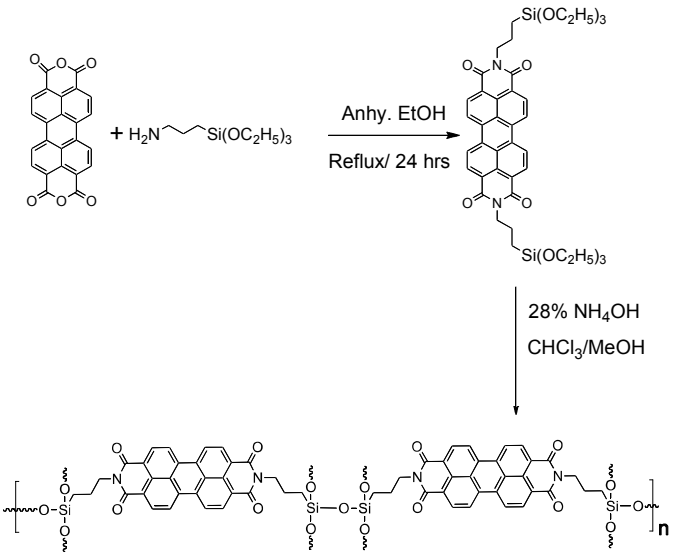

Scheme 1: Preparation of Poly-PDIB-SSQ nanoarrays by base-catalysed hydrolysis and condensation method.

As previously reported,[24] the perylenediimide-bridged-triethoxysilane precursor (PDIB-silane) was prepared by condensation of 3,4,9,10-tetracarboxyanhydrideperylene with 3-aminopropyltriethoxysilane in anhydrous ethanol. The polymerization of the PDIB-silane was performed in a 1:1 ratio of chloroform and methanol solution in the presence of ammonium hydroxide as a base and is depicted in **Scheme 1**. In a typical procedure, freshly prepared PDIB-silane was dissolved in chloroform solution (10 mg/mL) and placed in a clean vial after filtering through a 0.45µm filter. Two distinct layers (red colored bottom layer and colorless upper layer) were formed just after the addition of methanol/NH_4OH solution. The polymerization was induced by the addition of the alcohol-base solution resulting an aggregated light red suspension in the upper layer and a translucent red colored bottom layer in few minutes. However, this time interval could be longer if the bottom layer was not disturbed by the addition if methanol. **Figure 1** shows optical photographs capturing the visual changes of the polymerization and self-assembly process over different time intervals. After 24 hours of reaction time, a solution with light yellow color to dark red color from top to bottom was observed. The polymerization process was continued up to 48 hours to yield a dark red homogeneous suspension and was analyzed by electron microscopy. The SEM images confirmed the complete formation of nanostructures with lengths of up to 80 µm for the reaction with the base concentration of 14.4 mmol/mL (Entry II in the **Table 1**) whereas in other two cases (Entry I & III in **Table 1**) random aggregates, nanoparticles, and featureless structures were abundant (see **Figure 2**). At this stage, the solution was allowed to evaporate slowly at steady rate to yield crystalline sticks grown from sheets along the walls and up straight from the bottom of the vial (see **Figure S1**). The post purification of polymer nanoarrays was performed by centrifuging the suspension after 48 hours of reaction time, followed by repeating the two-solvent aggregation and slow evaporation method with no base (see experimental section for detail procedure).

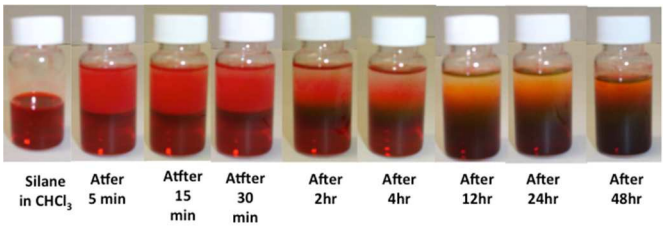

Figure 1: A series of optical photographs detailing the formation of poly-PDIB-SSQ nanoarrays.

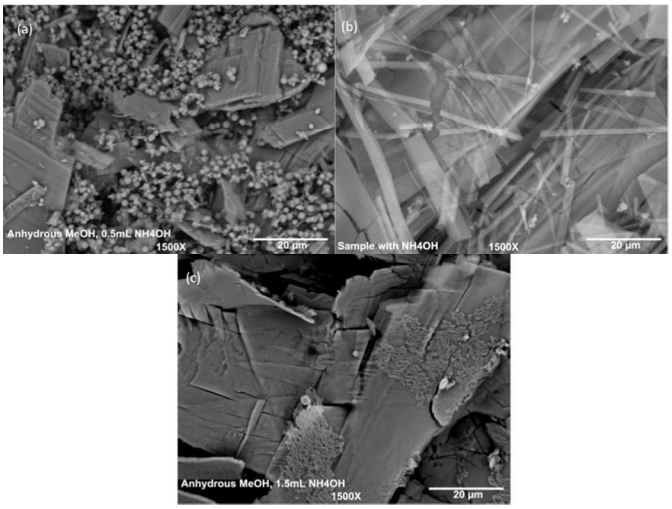

Figure 2: SEM images of Poly-PDIB-SSQ nanostructures taken after 48 hours of reaction time for three different base concentrations; (a) 7.2 mmol/mL, (b) 14.4 mmol/mL, and (c) 21.6 mmol/mL).

Table 1 summarizes the reaction conditions and dimensions of nanoarrays prepared in three different base concentrations. The repetitive reactions were performed and confirmed that the optimum base concentration for the formation of nanoarrays was 14.4 mmol/mL. We observed that at higher base concentration (21.6

mmol/mL), formation of random and featureless structures was more pronounced during the polymerization process whereas nanoparticles with sheet-like structures were formed at lower base concentration (7.2 mmol/mL). These morphology changes during the polymerization process clearly suggest that optimum base concentration is critical for controlling the formation of organized nanoarrays. The elemental analysis of the polymerized product confirmed the partially cross-linked poly-PDI-bridged silsesquioxane structure with residual ethoxy groups. The incomplete condensation is typically common in base catalyzed hydrolysis of alkoxysilanes for the preparation of poly silsesquioxanes as the percent of hydrolysis depends on the base concentration as we observed in our previous work.[24,25] The base catalyzed condensation usually has less condensing ability compared to acid catalyzed hydrolysis on silanols with electron donating groups.[29] The experimental percentages of carbon and hydrogen content were 1.08% and 0.64% higher than the calculated contents of carbon and hydrogen for fully condensed formula of R-Si_2O_3 (R= $C_{30}H_{20}N_2O_4$). Since in our case, the difference in carbon and hydrogen content agrees well with the structural formula with a residual ethoxy unit incorporated, the estimated degree of hydrolysis is five ethoxy reactive sites per PDI unit. Therefore, the formula of the polymer structure is a silsesquioxane network with the formula of R-Si_2O_3 where R is $C_{32}H_{25}N_2O_4$. MALDI-TOF-MS analysis of polymer revealed the molecular weight distribution with four peaks of higher *m/z* [M^-] at 2274, 2393, 2973, and 3120. These spectral traces confirmed five maximum repeating units of PDI per polymer chain with respect to the fully hydrolyzed monomer molecular peak of m/z at 591(see **Figure S2**).

Table 1: Reaction conditions and Morphology description of Poly-PDIB-SSQ nanostructures.

Entry #	NH_4OH concentration (mmol/mL)	Morphology description
I	7.20	Mostly nanoparticles and short nanoarrays (length from 10 µm to up to 55 µm with width ranging from 80-200 nm).
II	14.4	Long nanoarrays and sheets length up to 80 µm with width ranging from 60 – 200 nm
III	21.6	Few nanoparticles (100 -200 nm in size), random aggregates, and featureless structures

*The concentration of PDIB silane precursor used for each reaction is 10 mg/mL in chloroform solution.

Further characterization using FT-IR spectroscopy (**Figure S3**) confirmed the presence of characteristic bands for the formation of Si-O-Si bonds and the retention of Si-C linkages during the base-catalyzed polymerization. The alkyl chains -CH and diimide carbonyl stretching vibrations were observed at 2993-2885 and 1692 cm^{-1}, respectively. The presence of aromatic C-C stretching (1593-1553 cm^{-1}) and N-C vibrations (1440 cm^{-1}) further supports the successful retention of perylenediimide units to the silsesquioxane core. The well-defined absorption at 1343-1253 cm^{-1} confirms the presence of Si-C bonds in Si-PDI units. The absorption of Si-O-Si was observed at 1098-1016 cm^{-1}, suggesting the formation of a silsesquioxane network.

The influence of solvent processing and recrystallization on the morphology of nanoarrays was evaluated by re-dissolving the crude crystalline solid in a 1:1 mixture of chloroform and methanol followed by either drop casting or spin coating onto a glass substrate. Thin films were characterized by SEM and fluorescence optical microscopy. SEM images showed long thick stack of poly-PDIB rods like structures, having widths ~ 100-200 nm and lengths ~ 60-80 µm (**Figure 3a-b**). The longer lengths of these arrays suggest that crystallization initializes by individual nucleation sites to have well-defined interchain packing of PDI units within the silsesquioxane network, allowing the formation of micrometer lengths structures. Further characterization of a spin-coated sample of nanoarrays by fluorescence optical microscopy using a Rhodamine filter (excitation wavelength - 545 nm) confirmed incorporation of polymerized PDI units (Figure 3c-d). These post-processing results strongly support the formation of organized one-dimensional polymer nanoarrays via in-situ covalent synthesis.

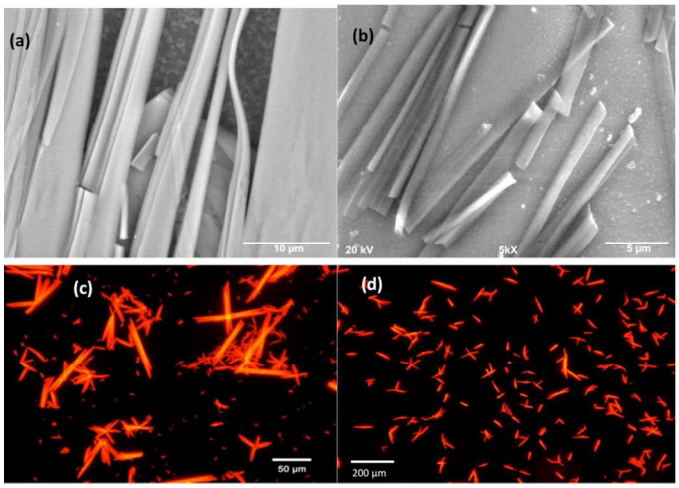

Figure 3: SEM images (a-b) and fluorescence optical microscopy images (c-d) of Poly-PDIB-SSQ nanoarrays after solvent processing.

SAXS characterization of Poly-PDIB nanoarrays confirmed their crystallinity and polymer chain ordering (**Figure 4**). The XRD pattern shows well-resolved multiple orders of Bragg peaks correspond to the Miller indices of (*h00*), (*0k0*) and (*00l*), where (h, k, *l are 1,2,3..*). The first (*001*), third (*003*), and fourth (*004*) Bragg peaks of (*00l*) were easily detected at 2θ angles of 3.56°, 10.56°, and 14.15° but the second Bragg peak (*002*) was not observed. The lower 2θ angle was observed for the first order (*001*) reflection compared to the literature reported value ($2\theta_{(001)}$ = 5.01°) for typical aggregated molecular PDIs.[30] However, such decrease in the first order reflection

angle was previously reported for self-assembled PDI-nanobelts.[9] The lower $2\theta_{(001)}$ is indicative of an increased interlamellar spacing due to the formation of silsesquioxane network upon hydrolysis.

The interchain separation distance $d_{[001]}$ is 24.8 Å and is in agreement with the interchain packing distance of self-assembled molecular PDI nanobelts reported in the literature.[9] Using the spacing of (*001*) combined with the spacing of its two higher order reflections (*003*) and (*004*), the possible ordering of PDI cores within the silsesquioxane network could be assigned to the layer by layer ordering where the layer of PDI cores is separated from the next layer of PDIs by the siloxane network as depicted in **Figure 5**.

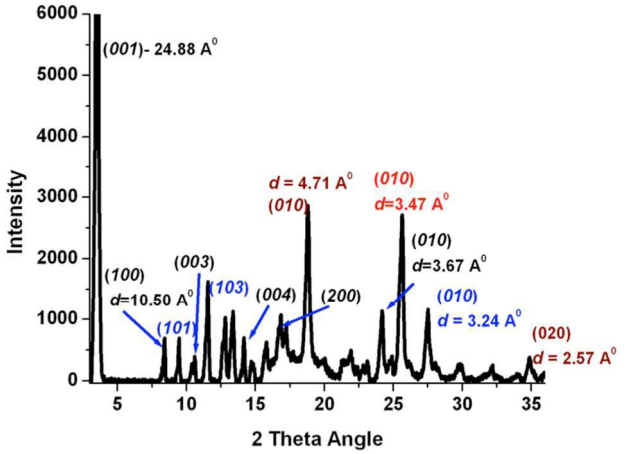

Figure 4: SAXS diffraction pattern of Poly-PDIB-SSQ nanoarrays.

The first and second order reflections of (*h00*) corresponding to the ordering of perylene cores within a layer of polymer chains were also identifiable at 2θ angles of 8.41° and 16.82. The interchain distance $d_{[100]}$ measured is 10.5 Å, which is close to the perylene core width of 9.2 Å.[31] This suggests that the most probable ordering of the PDI cores is edge-to edge as shown in **Figure 5** due to the large interdigitation caused by the sterically hindered siloxane network. The similar ordering of perylene cores was previously reported for columnar stacks of alkyl substituted perylenediimides liquid crystals having the (*100*) cell parameter distance of 10.3 Å.[31] The Miller indices (*101*) and (*103*) assigned to the peaks found at 9.45° and 11.57° further evidence that the ordering of polymer layers is correlated to the edge-to-edge ordering of PDIs.

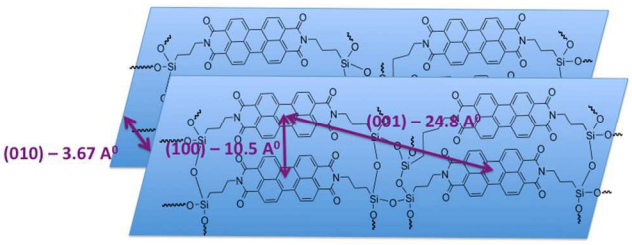

Figure 5: Schematic representation of possible ordering of polymer nanoarrays according to X-ray diffraction pattern.

Four different (*010*) out-of-plane reflections correspond to π-π stacking interactions were also observed in the XRD pattern. The first (010) reflection at 18.80° shows its second order reflection at 34.85° and the *d*-spacing was 4.71 Å to 2.57 Å respectively. The reduced d-spacing indicates much closer packing of polymer chains along the (*010*) plane. The second, third, and fourth reflections with d-spacing of 3.47 Å, 3.67 Å, and 3.24 Å confirm the presence of the π-π stacking of neighbouring, cofacially stacked perylene cores which results in the formation of nanoarrays. The thin film UV-visible absorption studies discussed later on further evidence the cofacial ordering of polymer chains in neighbouring stacks. Overall, the reduction in π-π stacking distance from 4.71 Å to 2.57 Å indicates the closely packed polymer layers along the four different (*010*) planes.

Characterization of poly-PDIB-nanoarrays by absorption and fluorescence emission spectroscopy in chloroform solution (Figure 6) shows characteristic spectral features similar to molecular PDI. The absorption spectrum confirmed three pronounced peaks with a shoulder at 425 nm, which corresponds to the 0-0, 1-1, 0-2, and 0-3 electronic transitions from left to right respectively.[30,32]

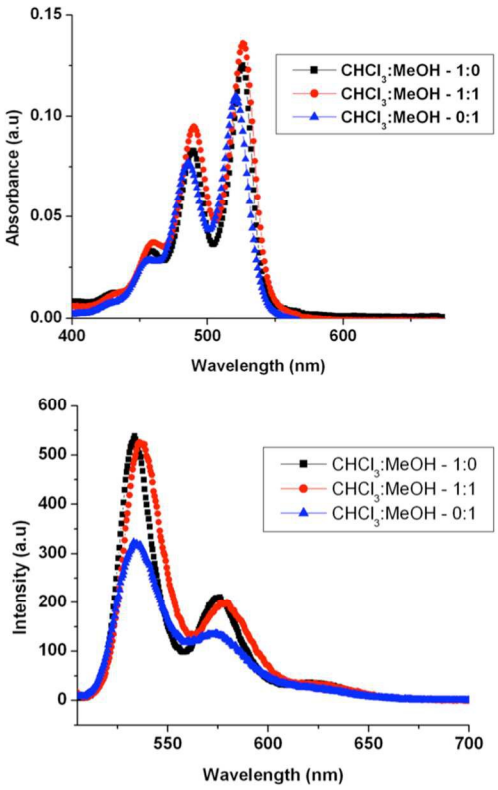

Figure 6: UV-visible absorption (top) and PL emission (bottom, excited at 497 nm) spectra of poly-PDI-SSQ nanoarrays in $CHCl_3$: MeOH ratios.

The fluorescence spectrum in 100% (v/v) chloroform solution depicts the similar spectral features in a mirror image of the absorption with some overlapping between longer wavelength absorption band and the shorter wavelength emission band. This overlapping is typical for closely packed PDI systems as reported previously.[30,32]

The absorption spectrum of poly-PDIB-SSQ nanoarrays in chloroform ($CHCl_3$) to methanol (MeOH) 1:1 solvent mixture shows pronounced electronic transitions from ground state to higher levels of electronic states (0-1, 0-2, and 0-3) with a rather weak shoulder from the 0-0 transition. Such spectral changes imply strong molecular packing between the polymer chains, similar to the spectral signatures reported for self-assembled molecular PDI nanobelts.[9] Poly-PDIB-SSQ nanoarrays showed complete aggregation in methanol ("poor" solvent) due to the limited solubility. The overall intensity of three absorption peaks somewhat reduced with slight blue shift. However, there is no sign of a pronounced absorption band emerging at longer wavelength (around 565 nm) that corresponds to the formation of π-π interactions in co-facial configuration of molecular stacking.[8,9,19] The fluorescence spectra taken in 1:1 and 0:1 chloroform to methanol solutions show slight red shifts (~5 nm) of emission maxima at 537 nm and 577 nm with no fluorescence quenching, which supports the lack of co-facial π-π interaction in "aggregated" form of poly-PDIB-SSQ nanoarrays in solution phase. However, a slight decreased in emission was observed in 0:1 chloroform: methanol mixture due to limited solubility resulting in aggregation of polymer chains.

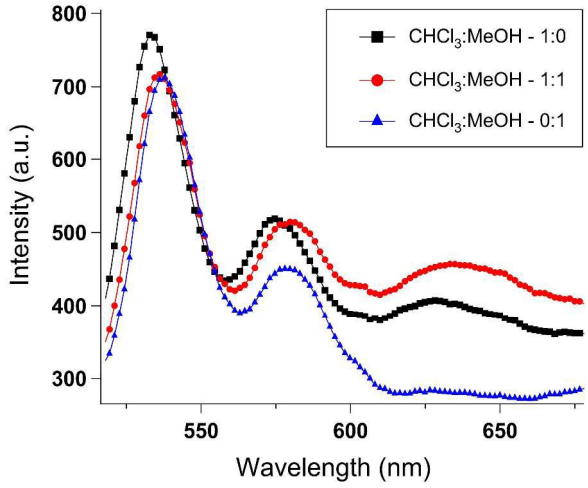

Figure 7: Thin film PL emission (excited at 485 nm) spectra of poly-PDIB-SSQ nanoarrays from 1:0, 1:1, and 0:1 $CHCl_3$:MeOH solutions.

The fluorescence emission spectra of poly-PDIB-SSQ nanoarray thin films spin coated from 1:0, 1:1, and 0:1 $CHCl_3$:MeOH solutions are shown in **Figure 7** and exhibit similar spectral features as their solution phase emission spectra. The shoulder peak at 630 nm was noticeable in thin films prepared from 1:0 and 1:1 solutions compared to that of in 0:1 thin film. Although considerable fluorescence quenching was not observed in all three cases, thin film absorption spectra (**Figure S4**) showed dramatic changes in spectral maxima at shorter wavelength with a pronounced absorption band also emerging at longer wavelength (~570 nm). The shorter wavelength absorption peaks that correspond to 0-1 and 0-2 electronic transitions are attributed to π-π interactions within the closely packed polymer chains. The longer wavelength band confirmed the presence of co-facial π-π interaction in solid state suggesting that thin films show similar structural morphology as crystalized polymer nanoarrays. The co-facial π-π interactions observed in thin films is in agreement with the co-facial ordering suggested from the powder diffraction data. Excited state lifetimes in solution and solid state are in agreement with their characteristic optical signatures (see **Figure 8**). The nanoarrays in 1:0 and 1:1 $CHCl_3$:MeOH solutions showed longer excited state lifetimes than those in their corresponding thin films due to closely packed nature of polymer chains in thin films. Interestingly, the excited state lifetimes of the 0:1 $CHCl_3$:MeOH solution was nearly identical to that of its corresponding thin film (3.8 ns vs 3.4 ns, respectively) suggesting that there are some similarities of polymer chain packing in "aggregated" form in solution phase and thin films. This behaviour also coincides with the lack of a pronounced shoulder at 630 nm in emission spectra of both solution and thin film in Figure 5 and Figure 6 respectively.

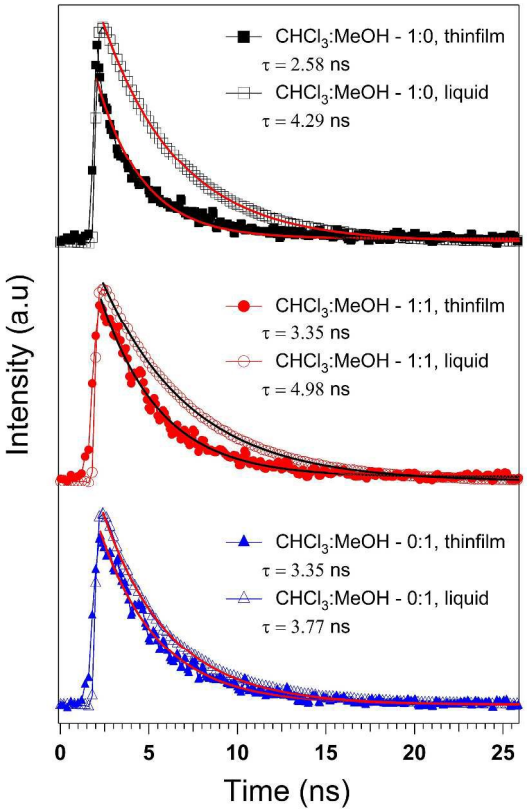

Figure 8: Excited state emission curves of poly-PDI-SSQ

nanoarrays in solution and in thin films created from 1:0, 1:1, and 0:1 $CHCl_3$:MeOH solutions.

In order to confirm the semiconducting behaviour of poly-PDIB-SSQ nanoarrays, electrical conductivity of polymer thin films were evaluated by spin coating the recrystallized polymer sample onto glass substrate. Test diodes with the configuration of ITO/poly-PDIB-SSQ/Ca-Al were fabricated. As shown in **Figure S5 (a)**, IV curve of a test device of poly-PDIB-SSQ shows the characteristic organic semiconducting curve with the open circuit voltage (V_{OC}) of 0.25 V. The asymmetrical nature of the curve is attributed to the difference in the work functions of electrodes. Electrical conductivities for both poly-PDIB-SSQ nanoarrays and the silane precursor were measured from their IV curves and conductivities were compared. The conductivity vs voltage curves are depicted in **Figure S5 (b)**. The electrical conductivity of poly-PDIB-SSQ was 0.48 x 10^{-3} S/cm, which is lower than the conductivity of its monomer (1.26 x 10^{-3} S/cm). The lower conductivity of poly-PDIB-SSQ nanoarrays evidences that the ordering of PDI units within the silsesquioxane network has impacted on electrical properties.

Conclusions

We have developed a in-situ covalent synthesis method to prepare crystalline nanoarrays from a n-type semiconducting polymer derived from poly(perylenediimide silsesquioxanes). These structures have dimensions of 100-200 nm in width and 60-80 μm in length as determined by SEM. SAXS confirmed their crystallinity and showed well-resolved Bragg reflections with multiple (*010*) out-of-plane reflections. Fluorescence spectroscopic signatures in an aggregated state in solution (1:1 $CHCl_3$:MeOH) show a slight red shift (~5 nm) compared to the solvated polymer with no fluorescence quenching. Interestingly, no distinct spectroscopic shift in absorption was observed upon aggregation in solution. In thin films, however, aggregation appears to play an important role in the photophysics of nanoarrays. Thin films of polymer nanoarrays show typical semiconducting behaviour with the electrical conductivity of 0.48 x 10^{-3} S/cm. This covalent synthesis followed by solvent-based crystallization of semiconducting polymers into organized nanostructures offers new insight for the preparation of novel 1D polymer nanoarrays. Nonetheless, research findings described here ultimately will benefit for the design of novel polymeric nanostructures having improved electronic properties for solar cells and other applications of conjugated polymer materials.

Experimental

Materials. 3,4,9,10-tetracarboxyanhydrideperylene, anhydrous methanol (99% purity), and Ammonium hydroxide (28%) were purchased from Aldrich chemicals. 3-aminopropyltriethoxysilane was purchased from Alfar Aesar and used as received. Unless otherwise specified, all chemicals were used as received.

Characterization. Proton NMR spectra were recorded on a 500 MHz Jeol using $CDCl_3$ as a solvent for the silane precursor. FTIR spectra were measured using a Perkin-Elmer Spectrum One FT-IR spectrometer equipped with a universal ATR sampling accessory. Mass spectra were acquired by the University of Kentucky Mass Spectrometry facility. Matrix-assisted laser desorption ionization mass (MALDI-TOFMS) spectra were obtained on a Bruker Daltonics (Billerica, MA) Ultraflextreme time-of-flight mass spectrometer with SmartBeam II Nd:YAG/355 nm laser operating at 200 Hz and laser focus set to "small" focus setting. Laser attenuation was optimized to obtain the best signal-to-noise (S/N) ratio, keeping maximum resolution. The sandwich method of sample preparation was employed with the matrix of ∝-cyano-4-hydroxycinnamic acid. The photophysical properties in solution were performed on fluorescence spectrometer (Perkin Elmer LS 55) and UV-visible spectrometer (Perkin Elmer, Lambda 35). Scanning electron microscopy (SEM) observations were performed on a 100CX JEOL at 80 keV. Thin film emission spectra and excited state lifetimes were acquired using a Nikon Eclipse TE2000-U inverted microscope with a 1.4 numerical aperture objective and a 485 nm ps pulsed diode laser with EMCCD camera detection (Princeton Instruments ProEM 1024). Solid state (concentrated thin film) absorption spectra were acquired using a Agilent Technologies Cary Series UV-Vis-NIR Spectrophotometer.

Typical Procedure for the preparation of poly-PDIB-SSQ nanoarrays: 50 mg (0.063 mmol) Freshly prepared perylenediimide-bridged silane (50.0 mg, 0.063 mmol) was dissolved in 5.0 mL of chloroform and then sonicated for one minute. The solution was filtered through a 0.45 μm syringe filter into a 20 mL vial. In a separate vial, 4.0 mL methanol and 1.0 mL ammonium hydroxide were mixed and were added gently to the first vial with no disturbance to the silane solution in the vial. Unless the bottom layer was disturbed in which case the top layer would take on an opaque red color, the methanol ammonium hydroxide solution formed a clear top layer (see Figure S1(a)) and the perylenediimide bridged silane in chloroform comprising a translucent red lower layer. The interface between these two layers was opaque and red, growing overtime until no clear distinction could be made between the layers. After 48 hours, a dark red homogenous suspension was obtained. At this stage solution was allowed to evaporate slowly to yield long red color needles in the lower portion of the vial as shown in Figure S1 (b). FTIR stretching (cm^{-1}): 2993-2885 (C-H stretching of alkyl chains), 1691 (diimide carbonyl stretching), 1594-1647 (aromatic C-C stretching), 1440 (N-C stretching from perylenediimide), 1379-1250 (Si-C stretching), 1098-1016 (Si-O-); MS (MALDI-TOF, negative): *m/z* = 2274, 2393, 2973, and 3120 [M^-]; Elemental analysis (%): Experimental- C 63.56, H 4.14, N 4.70, Si 9.31; Calculated (assuming product was fully hydrolysed)- C 62.48, H 3.50, N 4.86, Si 9.74.

Post purification of polymer nanoarrays: The suspension obtained after 48 hours of reaction time was centrifuged and washed with methanol to yield a red solid. The wet solid was

dissolved in minimum volume of chloroform in a vial and equal volume of methanol was slowly added to form two layers. The solution was tightly capped and kept with no disturbance. After 48 hours, the solution was allowed to evaporate slowly to yield crystals.

Electrical Characterization Measurements: The thin-film devices were prepared on glass/ITO substrates. The substrates were subsequently cleaned in 2- propanol and acetone in an ultrasonic bath for 15 minutes each. As a first step, the sample dissolved in chlorobenzene (10 mg/mL) was spin coated to give a film thickness of 300-400 nm under inert atmosphere. The substrates were transported into vacuum evaporator and a layer of aluminium (~50 nm) was thermally evaporated on top of the sample layer with a coating of 2 x 6 mm through a mask. The final devices were transferred to a glass chamber under a stream of nitrogen gas. The chamber was sealed for device characterization while maintaining the temperature of the devices at room temperature. The IV curves of the devices were measured using a Keithley 2400 source meter that connected to a PC supported with LabView. Conductivities were obtained from IV curves and plotted against sweeping voltage.

Acknowledgements

Financial support for this work is provided, in part, from the Department of Chemistry and Office of Research at Western Kentucky University, the Kentucky Science & Engineering Foundation (COMMFUND-1385-RFP-014), and from the National Science Foundation (CHE-0955550 and EPS-0903787). The authors gratefully acknowledge Dr. Jack Goodman at University of Kentucky for MALDI-TOF MS analysis, Dr. John Andersland for TEM support, Dr. Quentin Lineberry for TGA and XRD analysis, and Pauline Norris (from AMI) for elemental analysis.

Notes and references

a* Department of Chemistry, Western Kentucky University, Bowling Green KY 42101 Fax: 270-745-5361; Tel: 270-745-6238; E-mail: hemali.rathnayake@wku.edu.

b* Department of Chemistry & Biochemistry, University of Mississippi, MS 38677; E-mail:nhammer@olemiss.edu.

† Electronic Supplementary Information (ESI) available: experimental procedures are available in supporting information section. See DOI: 10.1039/b000000x/.

1. Green, J. E.; Wook Choi, J.; Boukai, A.; Bunimovich, Y.; Johnston-Halperin, E.; DeIonno, E.; Luo, Y.; Sheriff, B. A.; Xu, K.; Shik Shin, Y.; Tseng, H.-R.; Stoddart, J. F.; Heath, J. R.; *Nature* 2007, **445**, 414–417.
2. Duzhko, V.; Singer, K. D.; *J. Phys. Chem. C* 2007, **111**, 27–31.
3. Hill, J. P.; Jin, W.; Kosaka, A.; Fukushima, T.; Ichihara, H.; Shimomura, T.; Ito, K.; Hashizume, T.; Ishii, N.; Aida, T.; *Science* 2004, **304**, 1481–1483.
4. Briseno, A. L.; Mannsfeld, S. C. B.; Reese, C.; Hancock, J. M.; Xiong, Y.; Jenekhe, S. A.; Bao, Z.; Xia, Y.; *Nano Lett.* 2007, **7**, 2847–2853.
5. Praefcke, K.; Singer, D.; Kohne, B.; Ebert, M.; Liebmann, A.; Wendorff, J. H.; *Liquid Crystals* 1991, **10**, 147–159.
6. Tang, Q.; Li, H.; He, M.; Hu, W.; Liu, C.; Chen, K.; Wang, C.; Liu, Y.; Zhu, D.; *Adv. Mater.* 2006, **18**, 65–68.
7. Bendikov, M.; Wudl, F.; Perepichka, D. F.; *Chem. Rev.* 2004, **104**, 4891–4946.
8. Balakrishnan, K.; Datar, A.; Oitker, R.; Chen, H.; Zuo, J.; Zang, L.; *J. Am. Chem. Soc.* 2005, **127**, 10496–10497.
9. Balakrishnan, K.; Datar, A.; Naddo, T.; Huang, J.; Oitker, R.; Yen, M.; Zhao, J.; Zang, L.; *J. Am. Chem. Soc.* 2006, **128**, 7390–7398.
10. Sinks, L. E.; Rybtchinski, B.; Iimura, M.; Jones, B. A.; Goshe, A. J.; Zuo, X.; Tiede, D. M.; Li, X.; Wasielewski, M. R.; *Chem. Mater.* 2005, **17**, 6295–6303.
11. Gesquière, A.; Jonkheijm, P.; Hoeben, F. J. M.; Schenning, A. P. H. J.; De Feyter, S.; De Schryver, F. C.; Meijer, E. W.; *Nano Lett.* 2004, **4**, 1175–1179.
12. Schenning, A. P. H. J.; v. Herrikhuyzen, J.; Jonkheijm, P.; Chen, Z.; Würthner, F.; Meijer, E. W.; *J. Am. Chem. Soc.* 2002, **124**, 10252–10253.
13. Xu, B.; Xiao, X.; Yang, X.; Zang, L.; Tao, N.; *J. Am. Chem. Soc.* 2005, **127**, 2386–2387.
14. Garnier, F.; Hajlaoui, R.; Yassar, A.; Srivastava, P.; *Science* 1994, **265**, 1684–1686.
15. Hoppe, H.; Sariciftci, N. S.; *J. Mater. Chem.* 2006, **16**, 45–61.
16. Thompson, B. C.; Fréchet, J. M. J.; *Angew. Chem. Int. Ed.* 2008, **47**, 58–77.
17. Kroon, R.; Lenes, M.; Hummelen, J. C.; Blom, P. W. M.; de Boer, B.; *Polym. Rev.* 2008, **48**, 531–582.
18. Kiriy, N.; Bocharova, V.; Kiriy, A.; Stamm, M.; Krebs, F. C.; Adler, H.-J.; *Chem. Mater.* 2004, **16**, 4765–4771.
19. Würthner, F.; *Chem. Commun.* 2004, 1564–1579.
20. Datar, A.; Balakrishnan, K.; Yang, X.; Zuo, X.; Huang, J.; Oitker, R.; Yen, M.; Zhao, J.; Tiede, D. M.; Zang, L.; *J. Phys. Chem. B* 2006, **110**, 12327–12332.
21. Che, Y.; Datar, A.; Balakrishnan, K.; Zang, L.; *J. Am. Chem. Soc.* 2007, **129**, 7234–7235.
22. Zang, L.; Che, Y.; Moore, J. S.; *Acc. Chem. Res.* 2008, **41**, 1596–1608.
23. De Luca, G.; Liscio, A.; Maccagnani, P.; Nolde, F.; Palermo, V.; Müllen, K.; Samorì, P.; *Adv. Funct. Mater.* 2007, **17**, 3791–3798.
24. Rathnayake, H.; Binion, J.; McKee, A.; Scardino, D. J.; Hammer, N. I.; *Nanoscale* 2012, **4**, 4631–4640.
25. Rathnayake, H.; Wright, N.; Patel, A.; Binion, J.; McNamara, L. E.; Scardino, D. J.; Hammer, N. I.; *Nanoscale* 2013, **5**, 3212–3215.
26. Samitsu, S.; Shimomura, T.; Ito, K.; *Thin Solid Films* 2008, **516**, 2478–2486.
27. Grenier, C. R. G.; Pisula, W.; Joncheray, T. J.; Müllen, K.; Reynolds, J. R.; *Angew. Chem. Int. Ed.* 2007, **46**, 714–717.
28. Wang, H.-W.; Pentzer, E.; Emrick, T.; Russell, T. P.; *ACS Macro Lett.* 2014, **3**, 30–34.

29. Williams, E. A.; Cargioli, J. D.; Larochelle, R. W. J. Organomet. Chem. 1976, 108, 153–158.
30. Zhou, Z.; Brusso, J. L.; Holdcroft, S.; *Chem. Mater.* 2010, **22**, 2287–2296.
31. Struijk, C. W.; Sieval, A. B.; Dakhorst, J. E. J.; Dijk, M. V.; Kimkes, P.; Koehorst, R. B. M.; Donker, H.; Schaafsma, T. J.; Picken, S. J.; Craats, A. M. van de; Warman, J. M.; Zuilhof, H.; Sudhölter, E. J. R.; *JACS* 2000, **122**, 11057-11066.
32. Feng, J.; Liang, B.; Wang, D.; Wu, H.; Xue, L.; Li, X.; *Langmuir* 2008, **24**, 11209-11215.